Universality and scaling study of the critical behavior of the two-dimensional Blume-Capel model in short-time dynamics

Roberto da Silva*, Nelson A. Alves†, **and** J. R. Drugowich de Felício‡
Departamento de Física e Matemática, FFCLRP Universidade de São Paulo, Avenida Bandeirantes 3900, CEP 014040-901, Ribeirão Preto, São Paulo, Brazil
(February, 26, 2002)

In this paper we study the short-time behavior of the Blume-Capel model at the tricritical point as well as along the second order critical line. Dynamic and static exponents are estimated by exploring scaling relations for the magnetization and its moments at early stage of the dynamic evolution. Our estimates for the dynamic exponent, at the tricritical point, are $z = 2.215(2)$ and $\theta = -0.53(2)$.

Keywords: short-time dynamics, critical phenomena, dynamic exponent, Blume-Capel model, Monte Carlo simulations.

PACS-No.: 64.60.Fr, 64.60.Ht, 02.70.uu, 75.10.Hk

1. INTRODUCTION

Numerical simulation in the short-time regime has become an important tool to study phase transitions and critical phenomena. The reason is that universality and scaling behavior are already present in the dynamic systems since the early stages of their evolution [1,2]. Moreover, this kind of approach reveals the existence of a new and unsuspected critical exponent. As shown by Janssen *et al.* [1] on basis of renormalization group theory, if we tune the parameters at their critical values but with initial configurations characterized by nonequilibrium states, the time evolution of quantities like magnetization exhibit a polynomial behavior governed by an exponent θ, which is independent of the known set of static exponents and of the dynamical critical exponent z. This new exponent characterizes the so called "critical initial slip", the anomalous behavior of the magnetization when the system is quenched to the critical temperature T_c. Working with systems without conserved quantities, model A in the terminology of Halperin *et al.* [3], Janssen *et al.* found a scaling form for the moments of the magnetization, which sets soon after a microscopic time scale t_{mic}. Those relations have been confirmed in several numerical experiments [4–6]. For the kth moment of the magnetization, this scaling form reads

$$M^{(k)}(t, \tau, L, m_0) = b^{-k\beta/\nu} M^{(k)}(b^{-z}t, b^{1/\nu}\tau, b^{-1}L, b^{x_0}m_0)\,. \tag{1}$$

Here b is an arbitrary spatial scaling factor, t is the time evolution and τ is the reduced temperature, $\tau = (T - T_c)/T_c$. As usual, the exponents β and ν are the well-known static exponents, whereas z is the dynamic one. Equation (1) depends on the initial magnetization m_0 and gives origin to the new exponent x_0, the scaling dimension of the initial magnetization, related to θ by $\theta = (x_0 - \beta/\nu)/z$.

For a large lattice size L and small initial magnetization m_0, the system in its early stage presents small spatial and temporal correlation lengths, which may eliminate usual finite size problems. In this limit, if we choose the scaling factor $b = t^{1/z}$ [1,5,6] at the critical temperature ($\tau = 0$), we obtain

$$M(t, m_0) \sim m_0 t^{\theta} \tag{2}$$

from the scaling relation (1). The exponent θ has been calculated for the two-dimensional (2d) [5,7] and three-dimensional (3d) [7,8] Ising models, 2d 3-state Potts model [5], Ising model with next-nearest neighbor interactions [9] and Ising model with a line of defects [10]. In addition, this short-time universal behavior was found in irreversible models with synchronous [11] and continuous time dynamics [12]. In all of those cases, a positive value for θ has been found, that indicates a surprising initial increasing of the magnetization in the short-time regime $t_0 \sim m_0^{-z/x_0}$. This effect can be related to a "mean field" behavior since the system presents small correlation length in the beginning of

*E-mail: rsilva@dfm.ffclrp.usp.br
†E-mail: alves@quark.ffclrp.usp.br
‡E-mail: drugo@usp.br

the time evolution. Thus, when the system is quenched to the critical temperature T_c, it feels as being in an ordered state since $T_c < T_c^{MF}$ [13].

On the other hand, as shown by Janssen and Oerding [14], the behavior of a thermodynamic system is more complex at a tricritical point (TP) and the corresponding exponent θ may attain negative values.

At a tricritical point the magnetization shows a crossover from the logarithmic behavior $M(t) \sim m_0(\ln(t/t_0))^{-a}$ at short times $t << m_0^{-4}$ to $t^{-1/4}$ power law with logarithmic corrections, $M(t) \sim (t/\ln(t/t_0))^{-1/4}$ in 3 dimensions. The above behavior can be stated in the generalized form

$$M(t) = m_0 \left(\ln(t/t_0)\right)^{-a} F_M \left(\left(\frac{t}{\ln(t/t_0)} \right)^{1/4} (\ln(t/t_0))^{-a} m_0 \right) , \tag{3}$$

where $F_M(x) \sim 1$ or $F_M(x) \sim 1/x$, respectively for vanishing and large arguments. Below 3 dimensions it reduces to the scaling form

$$M(t) \sim m_0 t^{\theta} . \tag{4}$$

Here θ is the exponent related to the tricritical point of the relaxation process at early times and it is expected to assume negative values.

In this paper, we perform short-time Monte Carlo (MC) simulations to explore the critical dynamics of the 2d Blume-Capel model. We evaluate the dynamic exponents θ and z, besides the static exponents ν and β at the tricritical point. To the best of our knowledge this is the first time it is done numerically. We also estimate the dynamic exponents along the critical line. We observe a clear trend toward the values of z and θ for the corresponding 2d Ising values when the crystal field D becomes large and negative, indicating dynamic universality in the limit $D \to -\infty$.

The paper is organized as follows. In the next section we present the model and its phase diagram. Sec. III contains the main scaling relations and describes our short-time MC simulations. Results are presented for critical points on the second-order line. In Sec. IV, we explore the short-time dynamics to study the tricritical behavior. Sec. V contains a brief outlook and concluding remarks.

2. THE MODEL

The Blume-Capel [15] (BC) model is a spin-1 model which has been used to describe the behavior of $^3He - ^4He$ mixtures along the λ line and near the critical mixing point. Apart from its practical interest, the BC model has intrinsic interest since it is the simplest generalization of the Ising model ($s = 1/2$) exhibiting a rich phase diagram with first and second-order transition lines besides a tricritical point. In real systems tricritical points appear in $^3He - ^4He$ mixtures, such that when a small fraction of ^3He is added to ^4He, a critical line terminates at a concentration of ^3He approximately at 0.67. The BC model or its well known generalization, the Blume-Emery-Grifftihs model [16,17] was studied by mean-field approximation, real space and renormalization group schemes [18], Monte Carlo renormalization group approach [19] and finite-size scaling combined with conformal invariance [20–22]. The Hamiltonian of the two-dimensional model is

$$H = -J \sum_{<i,j>} S_i S_j + D \sum_{i=1} S_i^2 , \tag{5}$$

where $< i, j >$ indicates nearest neighbors on L^2 lattices and $S_i = \{-1, 0, 1\}$. The parameter J is the exchange coupling constant and D is the crystal field. We show its phase diagram in Fig. 1. Table I lists points on the second order critical line and the tricritical point where we have performed our simulations. Points in Table I were obtained from [23] and from a private communication of the authors in [22]. That table also contains our results for the corresponding critical and tricritical exponents.

We remark that along the critical line, this model presents a critical behavior similar to that of the Ising model. However, exactly at the tricritical point the exponents change abruptly. They are given by the dimensions of the irreducible representations of the Virasoro algebra [24,25] with central charge (conformal anomaly number) $c = 7/10$ [21]. In [20] finite-size scaling combined with conformal invariance permited to observe a smooth change between Ising-like and tricritical behavior. In finite systems, Ising-like behavior is reached only when $D \to -\infty$. In that limit $\eta/2(2 - 1/\nu) \to 0.125$ that is the exact value for the Ising model. In our short-time simulations the same kind of crossover behavior is observed for the dynamic exponents z and θ when we move along the critical line.

Table 1. Critical parameters and exponents for 2d Blume-Capel model.

D/J	k_BT/J	θ	z (Eq. (12))	z (Eq. (16))	$1/\nu$ (Eqs. (17) and (12))	$1/\nu$ (Eqs. (17) and (16))	β (Eq. (14))
critical points							
0	1.6950	0.194(3)	2.159(6)	2.1057(7)	0.97(2)	0.99(2)	0.134(2)
-3	2.0855	0.193(5)	2.156(5)	2.1276(5)	0.99(1)	1.00(1)	0.125(2)
-5	2.1855	0.187(5)	2.154(4)	2.1387(6)	0.99(3)	1.00(3)	0.125(4)
tricritical point							
1.9655	0.610	-0.53(2)	2.21(2)	2.215(2)	1.864(6)	1.86(2)	0.0453(2)

3. NON-EQUILIBRIUM SHORT-TIME DYNAMICS AT A CRITICAL POINT

In short-time MC simulations critical slowing down can be neglected. It happens because spatial and time correlation lengths are small in the early stages of evolution. On the other hand, we need to deal with several samples taken over independent initial configurations since the systems which are being simulated are far from equilibrium. In fact this approach requires calculation of average (over samples) magnetization and of its moments $M^{(k)}(t)$,

$$M^{(k)}(t) = \frac{1}{N_s L^{kd}} \sum_{j=1}^{N_s} \left(\sum_{i=1}^{L^d} \sigma_{ij}(t) \right)^k , \tag{6}$$

where $\sigma_{ij}(t)$ denotes the value of spin i of jth sample at the tth MC sweep. Here N_s denotes the number of samples and L^d is the volume of the system. This kind of simulation is performed N_B times to obtain our final estimates in function of t. In this paper, the dynamic evolution of the spins $\{\sigma_i\}$ is local and updated by the heat-bath algorithm.

A. The critical initial slip

The evolution of the kth moment of magnetization in the initial stage of the dynamic relaxation can be obtained from Eq. (1) for large lattice sizes L at $\tau = 0$ with $b = t^{1/z}$. This yields

$$M^{(k)}(t, m_0) = t^{-k\beta/\nu z} M^{(k)}(1, t^{x_0/z} m_0) . \tag{7}$$

By expanding the corresponding first moment equation for small m_0, we obtain Eq. (2) under the condition that $t^{x_0/z} m_0$ is sufficiently small, which sets a time scale $t_0 \sim m_0^{-z/x_0}$ [1,4,6] where that phenomena can be observed.

In Fig. 2a we present our results for the exponent θ at the critical point $k_BT_c/J = 1.695$ and $D_c/J = 0$, for lattice size $L = 80$ and 5 different initial magnetizations m_0. Our estimates for each $\theta = \theta(m_0)$ were obtained from $N_B = 5$ independent bins with $N_S = 10000$, for t up to 100 sweeps. Figure 2b illustrates the numerical evaluation of θ for $m_0 = 0.02$ from a log-log plot of the magnetization versus time. The linear fitting in Fig. 2a gives $\theta = 0.193(2)$ with goodness of fit [26] $Q = 0.72$.

Another method has been recently proposed by Tomé and de Oliveira [27] to evaluate θ. It avoids the sharp preparation of samples with defined and nonzero magnetization and the delicate numerical extrapolation $m_0 \to 0$. The method is based on the time correlation function of the total magnetization,

$$C(t) = \frac{1}{L^d} \left\langle \sum_{i=1}^{L^d} \sum_{j=1}^{L^d} \sigma_i(t)\sigma_j(0) \right\rangle . \tag{8}$$

Starting from random initial configurations the above correlation behaves as $C(t) \sim t^\theta$, which permits us to obtain the exponent θ from a log-log plot of $C(t)$ versus t. We obtained $\theta = 0.194(3)$ for $k_BT_c/J = 1.695$ and $D_c/J = 0$ choosing the time interval $[20 - 150]$ due to the highest value of Q ($Q = 0.99$). This value is in complete agreement with our above estimate of the exponent θ and it is consistent within error bars with previous results for the 2d Ising model. In table I we also present results for θ at several points of the critical line.

B. Dynamic critical exponent z

The observables in short-time analysis are described by different scaling relations according to the initial magnetizations. In particular, the second moment $M^{(2)}(t,L)$ in Eq. (6),

$$M^{(2)} = \frac{1}{L^{2d}} \left\langle \sum_{i=1}^{L^d} \sigma_i^2 \right\rangle + \frac{1}{L^{2d}} \sum_{i \neq j}^{L^d} \langle \sigma_i \sigma_j \rangle \ , \tag{9}$$

with $m_0 = 0$ behaves as L^{-d} since in the short-time evolution the spatial correlation length is very small when compared with the lattice size L. Thus, we arrive at [5,6]

$$M^{(2)}(t,L) = t^{-2\beta/\nu z}\, M^{(2)}(1, t^{-1/z} L) \sim t^{(d-2\beta/\nu)/z} \, . \tag{10}$$

This equation can be used to determine relations involving static critical exponents and the dynamic exponent z [6,28]. However, a way to evaluate independently the exponent z is through out the time-dependent fourth-order Binder cumulant at the critical temperature ($\tau = 0$),

$$U_4(t, L, m_0) = 1 - \frac{M^{(4)}(t, L, m_0)}{3 \left(M^{(2)}(t, L, m_0) \right)^2} \, , \tag{11}$$

which obeys the equation

$$U_4(t, L, m_0) = U_4(b^{-z} t, b^{-1} L, b^{x_0} m_0) \, . \tag{12}$$

If we set $m_0 = 0$, we eliminate the dependence on the exponent x_0 and the exponent z can be evaluated through scaling collapses of the generalized cumulant for different lattice sizes [4,29]. To match the Binder cumulants $U_4(t_1, L_1)$ and $U_4(t_2, L_2)$ obtained from two time series for lattice sizes L_1 and L_2, respectively, with $b = L_2/L_1$ ($L_2 > L_1$), we interpolate the series $U_4(t, L_1)$ to obtain $\widetilde{U}_4(b^{-z} t, L_1)$. Next, we define the function

$$\chi^2(z) = \frac{1}{t_f - t_i} \sum_{t=t_i}^{t_f} \left[\widetilde{U}_4(b^{-z} t, L_1) - U_4(t, L_2) \right]^2 \, , \tag{13}$$

where the best estimate for z corresponds to the one which minimizes $\chi^2(z)$.

In Fig. 3 we show the scaling collapses of the Binder cumulants for different lattice sizes. We have collapsed the following pairs of lattices $(L_1, L_2) = (10, 20), (20, 40)$ and $(40, 80)$. From the largest pair of lattices we obtained $z = 2.159(6)$ in the time interval $[50 - 1000]$. Our final error estimate is based on 25 different collapses obtained from $N_B = 5$ independent bins for each lattice size.

Another universal behavior of the dynamic relaxation process also described by Eq. (1) can be obtained with the initial condition $m_0 = 1$ [30–32]. This condition is related to another fixed point in the context of renormalization group approach. Thus, starting from an initial ordered state one obtains a power law decay of the magnetization at the critical temperature,

$$M(t) \sim t^{-\beta/\nu z} \, , \tag{14}$$

when we choose $b^{-z} t = 1$ in the limit of $L \to \infty$. Taking into account this relation, another method has been proposed [6] to estimate the dynamic exponent z. This approach uses the second cumulant

$$U_2(t, L) = \frac{M^{(2)}(t, L)}{(M(t, L))^2} - 1 \, , \tag{15}$$

which should take the simple form $U_2(t, L \to \infty) \sim t^{d/z}$. The advantage of this procedure is that curves for different lattices lay on the same straight line in a log-log plot without any re-scaling in time. However, this technique has not been successful in at least two well known models: the two-dimensional $q = 3$ Potts model [6] and the Ising model with three spin interactions in just one direction [10]. The reason for the above disagreement may be related to the behavior of the second term of r.h.s in Eq. (9) when $m_0 = 1$. We have proposed [33] that this behavior could indeed be obtained working with the ratio $F_2 = M^{(2)}/M^2$ with different initial conditions for each moment. As we know

the behavior of the second moment of the magnetization when samples are initially disordered ($m_0 = 0$) and also the time dependence of the magnetization when samples are initially ordered ($m_0 = 1$), we easily obtain

$$F_2(t) = \frac{M^{(2)}(t,L)\big|_{m_0=0}}{(M(t,L))^2\big|_{m_0=1}} \sim t^{d/z}\,. \tag{16}$$

A log-log plot with error bars for the critical point $k_BT_c/J = 1.695$ and $D_c/J = 0$ is presented in Fig. 4 for $L = 160$. We obtained $z = 2.1057(7)$ with $Q = 0.99$ in the range $[30 - 200]$, which does not agree with the value obtained from Eq. (12). However, as we move away from the tricritical point, the values of z obtained (Table 1) with Eq. (16) show a clear trend toward the expected value of the dynamic exponent z ($z = 2.1567(7)$) of the 2d Ising model [33]. On the other hand, the values obtained from the cumulant in Eq. (12) remain essentially the same along the entire critical line. It seems the cumulant U_4 is less sensitive to crossover effects than the mixed method.

C. Static exponents and universality class

The exponent $1/\nu z$ can be obtained by differentiating $\ln M(t, \tau, m_0)$ with respect to the temperature at T_c,

$$\left.\frac{\partial \ln M(t,\tau,L)}{\partial \tau}\right|_{\tau=0} \sim t^{1/\nu z}\,, \tag{17}$$

if we consider the scaling relation for the magnetization when the initial state of samples is ordered ($m_0 = 1$) [29].

Our results for νz were obtained through finite diferences at $T_c \pm \delta$ with $\delta = 0.001$. They rely on $N_B = 5$ independent bins with $N_s = 5000$ samples each for $L = 160$. The time interval $[80 - 200]$ corresponds to the range where the goodness of fit parameter attains its highest value ($Q = 0.99$).

In Fig. 5 we show the log-log behavior of the derivative $\partial_\tau \ln M(t)$ at $k_BT_c/J = 1.695$ and $D_c/J = 0$. In Table I we present our final estimates of $1/\nu$. The 6th column is obtained with the estimates of z from Eq. (12) (data in 4th column), while the 7th column corresponds to estimates for ν with values of z from Eq. (16) (data in 5th column).

Since we have already collected estimates for νz, it is straightforward to obtain estimates for β following Eq. (14). Our estimates of β are presented in the last column. Our values in Table I can be compared with theoretical predictions for an Ising like critical point ($1/\nu = 1, \beta = 1/8$).

4. RESULTS FROM SHORT-TIME DYNAMICS AT THE TRICRITICAL POINT

From the results presented in Refs. [1] and [14] we can describe the time dependence of the magnetization ($k = 1$) for the 2d Blume-Capel model as

$$M(t) \sim \begin{cases} m_0 t^{\theta}\,, \quad 0 < t < t_0\,, \quad \text{where } \theta \geq 0 & \text{critical} \\ t^{-\beta/\nu z}\,, \quad t_0 < t < t_I & \text{point} \\ \\ m_0 t^{\theta}\,, \quad 0 < t < t_0\,, \quad \text{where } \theta \leq 0 & \text{tricritical} \\ t^{-\beta/\nu z}\,, \quad t_0 < t < t_I & \text{point} \end{cases} \tag{18}$$

for an initial small magnetization m_0. Here t_I stands for the time before the system has reached the thermalization.

We also included in Table I our estimates for $\theta, z, 1/\nu$ and β at the tricritical point $k_BT_t/J = 0.610$ and $D_t/J = 1.9655$ working with lattice size $L = 80$.

In Fig. 6a we show the values of θ for 5 different initial magnetizations m_0 at the tricritical point and in Fig. 6b the time evolution of the magnetization for $m_0 = 0.08$ in a log-log plot. Our estimates for each $\theta(m_0)$ were obtained from $N_B = 20$ independent bins with $N_S = 10000$ samples, for t up to 80 sweeps. The linear extrapolation in Fig. 6a gives $\theta = -0.53(2)$ with goodness of fit $Q = 0.75$. The corresponding study with the time correlation function in Eq. (8) also gives $\theta = -0.53(2)$ with $Q = 0.99$ in the time interval $[20 - 80]$. The generalization of the dynamic scaling relation for the kth moment of the magnetization at a tricritical point can be written as [34]

$$M^{(k)}(t, \tau, g, L, m_0) = b^{-k\beta_t/\nu} M^{(k)}(b^{-z}t, b^{1/\nu}\tau, b^{\phi_t/\nu}g, b^{-1}L, b^{x_0}m_0). \tag{19}$$

It differs from the critical case by the scaling field g that measures the shunting line of critical point along of tangent transition line (at the tricritical point). The quantity ϕ_t is the known as the crossover exponent. At the criticality we have $\phi_t = g = 0$.

We show in Fig.7 scaling collapses of the cumulant $U_4(t, L)$ at the tricritical point, whose behavior is quite different of the corresponding one at a critical point (Fig. 3). Our first estimate based on Eq. (12) leads to $z = 2.21(2)$. This value was obtained from the pair of largest lattice sizes $L = 40$ and 80. The value remains the same when we consider the time interval $[10, 1000]$ or $[200, 1000]$. The second estimate for the dynamic exponent, based on Eq. (16) gives $z = 2.215(2)$. It was obtained from a larger lattice ($L = 160$) in the time interval $[30, 200]$, with $Q = 0.71$. We do not show the log-log plot of $F_2(t)$ in this case because it is quite similar to Fig. 4. We had to restrict the time interval, when compared with the U_4 calculation, in order to obtain acceptable values for Q. Here, in contrast to the estimates of z (4th and 5th column) at the critical points listed in Table I, both methods lead to the same numerical result.

The evaluation of static exponents ν and β at the tricritical point follows the same procedure as applied to the critical line. Estimates exhibited in Table I are in good agreement with results provided by conformal invariance $\nu = 9/5$ and $\beta = 1/24$.

Next, in order to study the influence of the local dynamics over the values of the exponents we recall the simulations with Glauber dynamics performed by de Alcantara Bonfim. Our estimates of $\beta/\nu z$ obtained from the decay of the magnetization (starting from initialy ordered state) is 0.0381(1) with the heat-bath dynamics while $\beta/\nu z = 0.0377(7)$ when updated following Glauber rules.

5. CONCLUSIONS

We have performed short-time Monte Carlo simulations to evaluate dynamic and static exponents at critical and tricritical points of the spin-1 Blume-Capel model. According to analytical predictions by Janssen and Oerding, a negative value for the new exponent θ was obtained for the tricritical point. The dynamic exponent z was estimated by colapsing the fourth-order Binder cumulant and also by the function $F_2(t)$ which explores time evolution of the magnetization starting from different initial conditions. The value of z was used to obtain the static exponents β and ν which resulted in good agreement with the exact results provided by the tricritical Ising model [21,24]. The dynamic exponents also were calculated along the critical line. Estimates for θ are in good agreement with known result for the 2d Ising model. However, near the tricritical point we found strong crossover effects on dynamical exponent z when using the recently proposed [33] technique based on mixed initial conditions. On the other hand, the fourth-order Binder cumulant is almost free from crossover effects.

Acknowledgments

R. da Silva and J. R. Drugowich de Felício gratefully acknowledge support by FAPESP (Brazil) and N.A. Alves by CNPq (Brazil). The authors deeply thank also to J. A. Plascak and J. C. Xavier for their communication about the values of critical points for $D < 0$ and DFMA (IFUSP) for the computer facilities extended to us.

---

[1] H. K. Janssen, B. Schaub and B. Schmittmann, Z. Phys. B **73**, 539 (1989).
[2] D. A. Huse, Phys. Rev. B **40**, 304 (1989).
[3] B. I. Halperin, P. C. Hohenberg and S-K. Ma, Phys. Rev. B **10**, 139 (1974).
[4] Z. B. Li, L. Schülke and B. Zheng, Phys. Rev. Lett. **74**, 3396 (1995).
[5] K. Okano, L. Schülke, K. Yamagishi and B. Zheng, Nucl. Phys. B **485** [FS], 727 (1997).
[6] B. Zheng, Int. J. Mod. Phys. B **12**, 1419 (1998).
[7] P. Grassberger, Phys. A **214**, 547 (1995).
[8] Z.-B. Li, U. Ritschel, B. Zheng, J. Phys. A: Math. Gen. **27**, L837 (1994).
[9] Y. E. AiJun, Pan ZhiGang, Chen Yuan and Li ZhiBing, Commun. Theor. Phys. (Beijing, China) **33**, 205 (2000).
[10] C. S. Simões and J. R. Drugowich de Felício, J. Phys. A **31**, 7265 (1998); T. Tomé, C. S. Simões and J. R. Drugowich de Felício, Mod. Phys. Lett. B **15**, 487 (2001); L. Wang, J. B. Zhang, H. P. Ying and D. R. Ji, Mod. Phys. Lett. B **13**, 1011 (1999).
[11] T. Tomé and J. R. Drugowich de Felício, Mod. Phys. Lett. B **12**, 873 (1998).
[12] J. F. F. Mendes and M. A. Santos, Phys. Rev. E **57**, 108 (1998).
[13] J.-B. Zhang, L. Wang, D.-W. Gu, H.-P. Ying and D.-R. Ji, Phys. Lett. A **262**, 226 (1999), and references therein.
[14] H. K. Janssen and K. Oerding, J. Phys. A: Math. Gen. **27**, 715 (1994).
[15] M. Blume, Phys. Rev. **141**, 517 (1966). H. W. Capel, Physica **32**, 966 (1966); **33**, 295 (1967); **37**, 423 (1967).
[16] M. Blume, V. J. Emery and R. B. Griffiths, Phys. Rev. A **4**, 1071 (1971).
[17] I. D. Lawrie and S. Sarbach, in *Phase Transitions and Critical Phenomena*, vol.9. Edited by C. Domb and J.L. Lebowitz, 1984 (Academic Press).
[18] A. N. Berker and M. Wortis, Phys. Rev. B **14**, 4969 (1976); T. W. Burkhardt, ibid. **14**, 1196 (1976).
[19] D. P. Landau and R. H. Swendsen, Phys. Rev. Lett. **46**, 1437 (1981).
[20] F. C. Alcaraz, J. R. Drugowich de Felício, R. Köberle and J. F. Stilck, Phys. Rev. B **32**, 7469 (1985).
[21] D. B. Balbão and J. R. Drugowich de Felício, J. Phys. A **20**, L207 (1987).
[22] J. C. Xavier, F. C. Alcaraz, D. Penã Lara and J. A. Plascak, Phys. Rev. B **57**, 11575 (1998).
[23] P.D. Beale, Phys. Rev. B **33**, 1717 (1986).
[24] D. Friedan, Z. Qiu and S. Shenker, Phys. Rev. Lett. **52**, 1575 (1984).
[25] J. L. Cardy, Nucl. Phys. B **270**, 186 (1986); B **275**, 200 (1986).
[26] W. Press *et al.*, *Numerical Recipes* (Cambridge University Press, London, 1986).
[27] T. Tomé and M. J. de Oliveira, Phys. Rev. E **58**, 4242 (1998).
[28] K. Okano, L. Schülke and B. Zheng, Foundations of Physics **27**, 1739 (1997).
[29] Z. Li, L. Schülke, B. Zheng, Phys. Rev. E **53**, 2940 (1996).
[30] D. Stauffer, Physica A **186**, 197 (1992).
[31] C. Münkel, D.W. Heermann, J. Adler, M. Gofman and D. Stauffer, Physica A **193**, 540 (1993).
[32] L. Schülke, B. Zheng, Phys. Lett. A **215**, 2940 (1996).
[33] R. da Silva, N. A. Alves and J. R. Drugowich de Felício, cond-mat/0111288.
[34] O. F. de Alcantara Bonfim, J. Stat. Phys. **48**, 919 (1987).

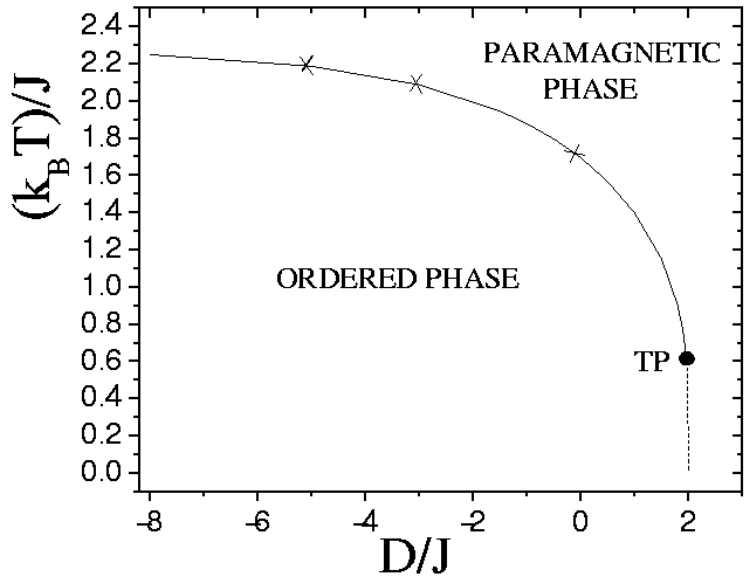

(Fig.1) 1. Phase diagram of the Blume-Capel model. The dashed curve is a first-order transition line and the solid is a second order one. These curves are connected by a tricritical point (TP). The marked points ($\times, \bullet$) correspond to the simulated values.

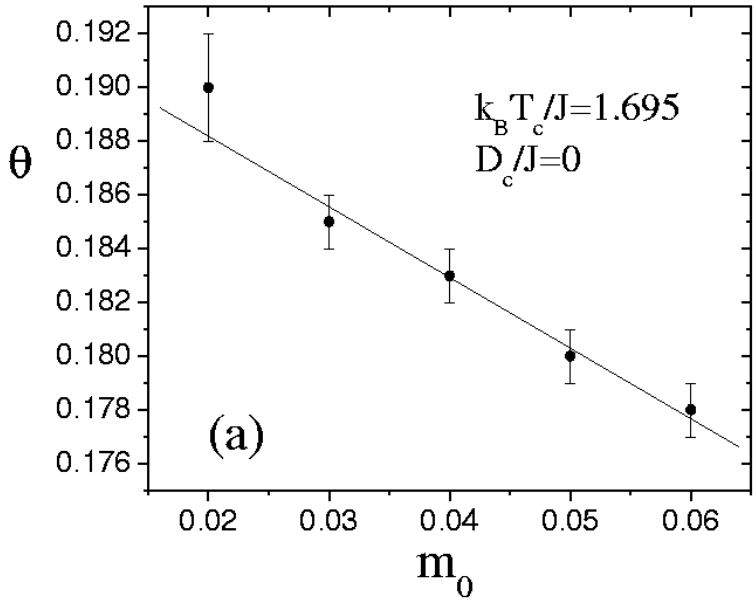

(Fig.2a) 2. Exponent θ in function of initial magnetizations m_0 for square lattices with $L = 80$. The straight line is a least-square fit to the data.

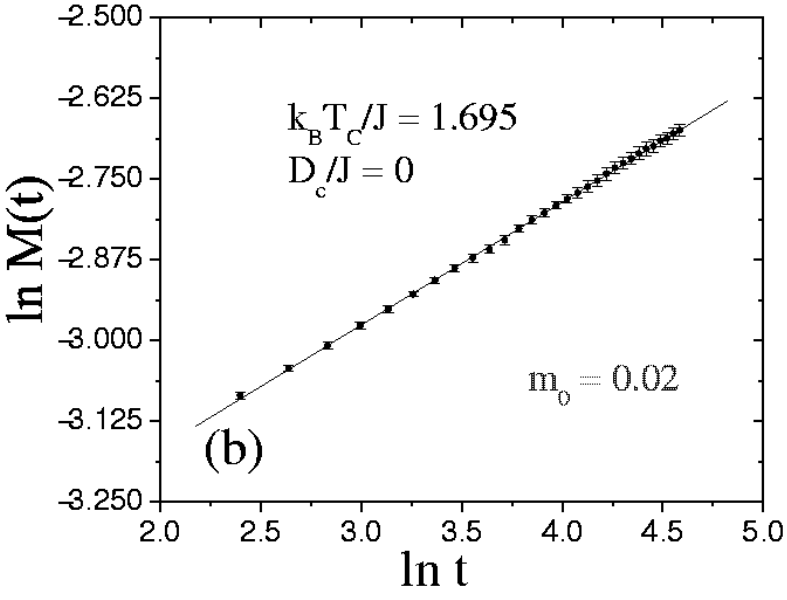

(Fig.2b) 3. Time evolution of the magnetization for $L = 80$ and $m_0 = 0.02$.

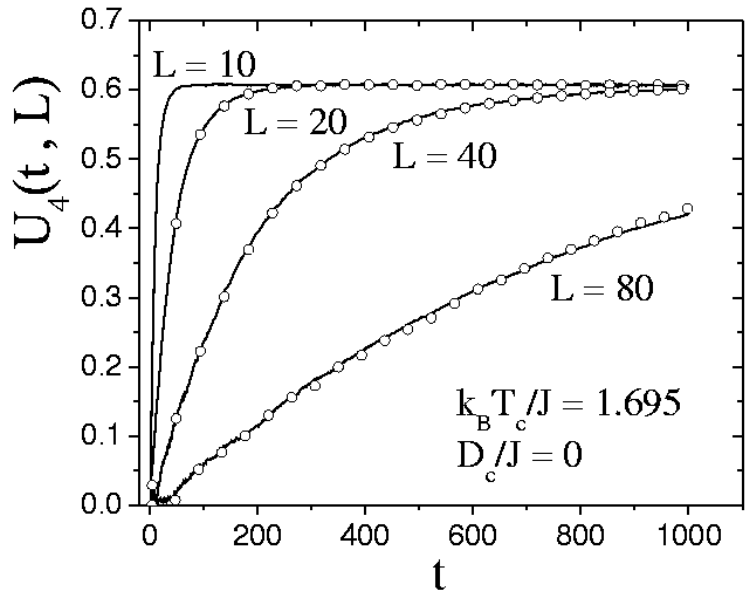

(Fig.3) 4. Cumulants $U_4(t, L)$ for $L = 10, 20, 40$ and 80 for initial magnetization $m_0 = 0$. The dots on the lines show the cumulants for lattice sizes $L/2$ rescaled in time with z given by Eq. (13).

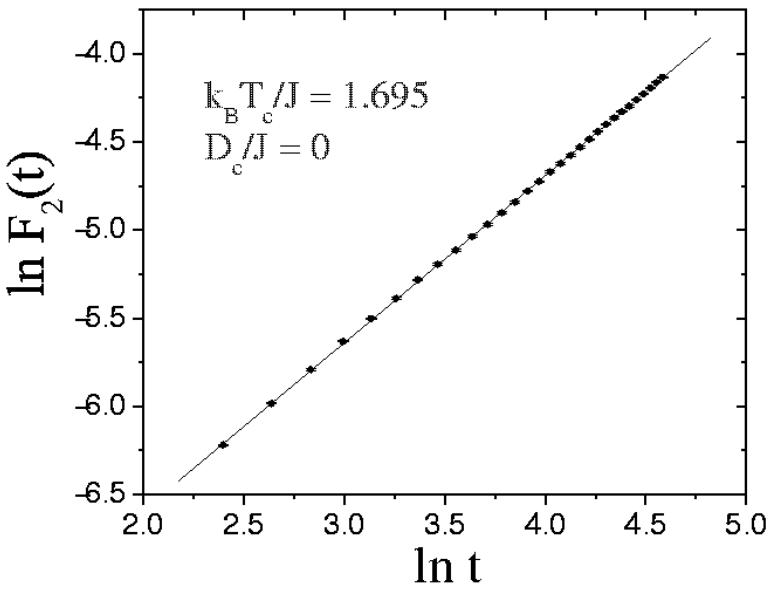

(Fig.4) 5. Time evolution of $F_2(t)$ for $L = 160$ with mixed initial magnetizations.

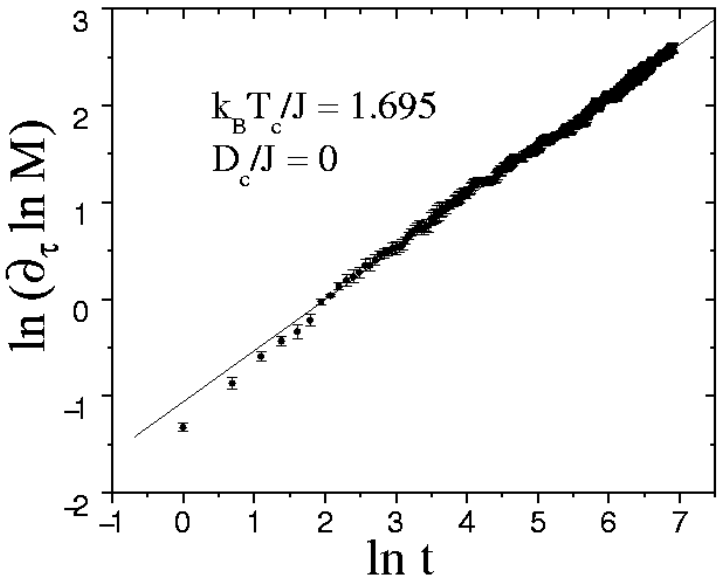

(Fig.5) 6. Time evolution of the derivative $\partial_\tau \ln M(t,\tau)|_{\tau=0}$ for $L = 160$ and initial magnetization $m_0 = 1$.

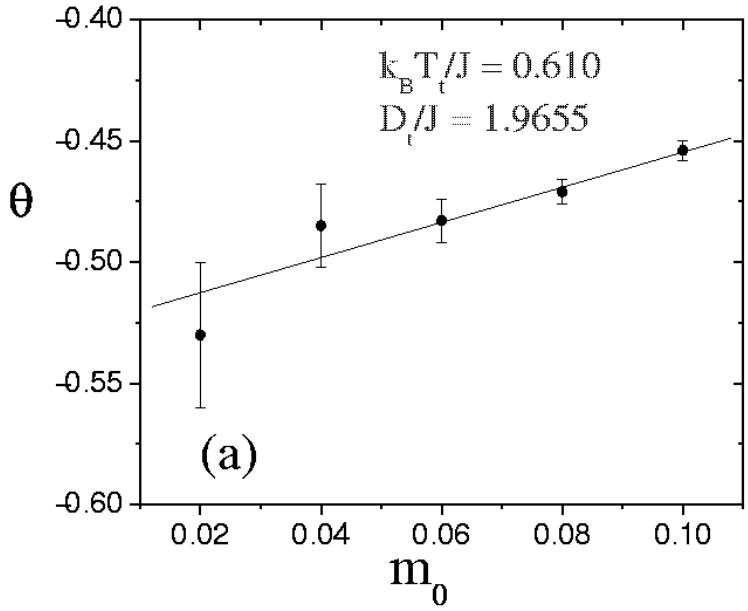

(Fig.6a) 7. Exponent θ in function of initial magnetizations m_0 for $L = 80$ at the tricritical point. The straight line is a least-square fit to the data.

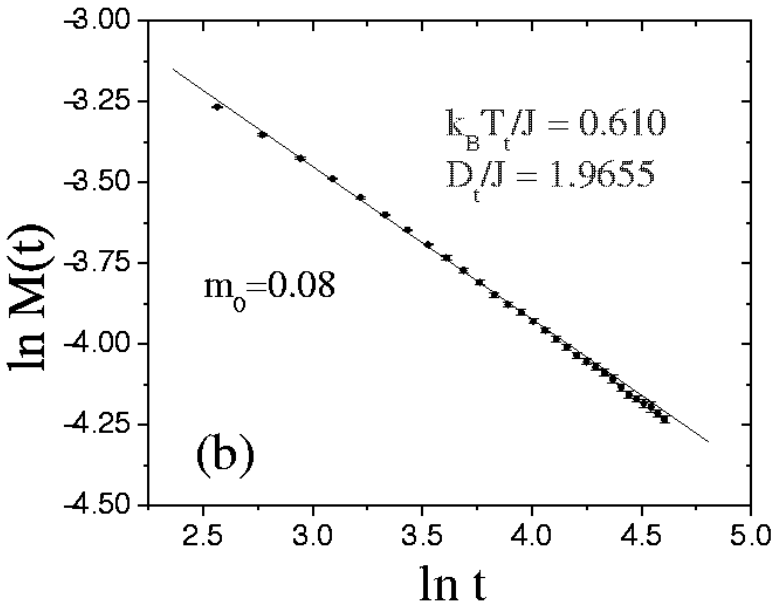

(Fig.6b) 8. Time evolution of the magnetization for $L = 80$ and fixed $m_0 = 0.08$ at the tricritial point.

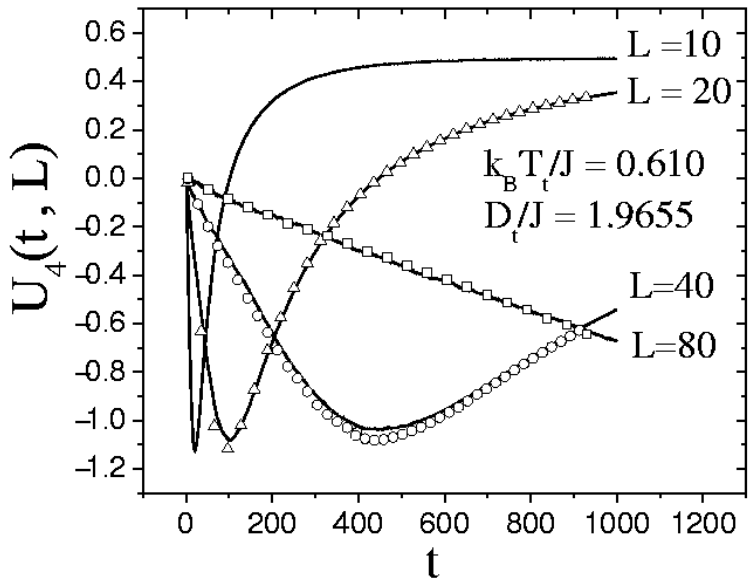

(Fig.7) 9. Cumulants $U_4(t, L)$ for $L = 10, 20, 40$ and 80 for an initial magnetization $m_0 = 0$ at the tricritical point. The dots on the lines show the cumulants with lattice sizes $L/2$ rescaled in time with z given by Eq. (13).